*J. King Saud Univ.*, Vol. 14, *Eng. Sci.* (2), pp. 199-209, Riyadh (A.H. 1422/2002)

# ANN Based Power System Stabilizers for Large Synchronous Generators

**Salah G. Foda**

*Department of Electrical Engineering, College of Engineering, King Saud University, P.O. Box 800, Riyadh 11421, Saudi Arabia*

(Received 04 November, 2000; accepted for publication 08 May, 2001)

**Abstract.** This paper presents an artificial neural network based power system stabilizer (ANNPSS) for excitation control for a large synchronous generator. The generator operates over a wide range of operating conditions and is subjected to different types of disturbances and emergency states. A 300 MW turbo-generator is used to generate appropriate training data for the ANN controller. Off-line simulations using a suitable conventional PSS to control the generator for different working conditions are used to generate training input-output pairs. A multi-layered back propagation (BP) ANN is utilised to design the ANN based controller where speed error deviation and the incremental change in machine terminal voltage are fed to the ANNPSS controller. The proposed ANNPSS and conventional PSS are compared and test results indicate that the ANN based controller is more adaptive and flexible than conventional stabilizers and show a good performance over a wide range of operating conditions and disturbances.

## Introduction

The automatic voltage regulator (AVR) is the keystone in the excitation system to control the terminal voltage of large turbo-generators. It also plays an essential role to control the reactive power and to enhance the machine stability. High gain AVR improves the dynamic limits of the generators. However, they can also introduce negative damping, especially in weakly coupled networks and consequently result in unstable operation. In order to overcome this problem, supplementary stabilizing signals should be introduced in the control circuit [1-4]. The main purpose of the stabilizing signals is to enhance system dynamics by producing a torque in phase with the generator speed. These stabilizing signals are usually derived by processing the speed signal through a suitable circuit called power system stabilizer (PSS) [5-9].

Artificial neural networks (ANNs) are rapidly gaining popularity among power system researchers. ANNs are extremely useful in the area of learning control. Consequently, the traditional adaptive control design has taken a new turn with the advent of ANNs [10]. ANNs are capable of learning from off-line simulation data and can then be trained to reflect the behaviour of the system under various operating conditions. In order to get the appropriate training data for ANN, the generating unit must be operated at first with a suitable PSS. In this paper, the off-line simulations are studied using a suitable conventional PSS to control the generator for different working conditions to get the generator input/output pairs that are then used as the ANN training data. The ANN is trained over a wide range of generator output ranging from 0.1-1.0 pu. Similarly, a wide spectrum of possible disturbances has been used for training. These disturbances cover the reference and infinite bus voltage disturbance in the range of + 0.05 pu, governor input, transmission line outage, and 3-phase faults on one circuit of the transmission lines connected to the generating unit [11-13]. The corresponding speed and voltage deviations of the generator were sampled at 20 ms intervals for control signal computation.

In the present work, two stabilizers, namely conventional and ANN-based stabilizers, are studied and compared to control an existing turbo-generator of 300 MW connected to an infinite bus through a transmission line (cf. Fig. 1). The test results indicate that the ANN-based stabilizer provides an improved performance compared to that of the conventional PSS over a wide range of operating conditions and disturbances.

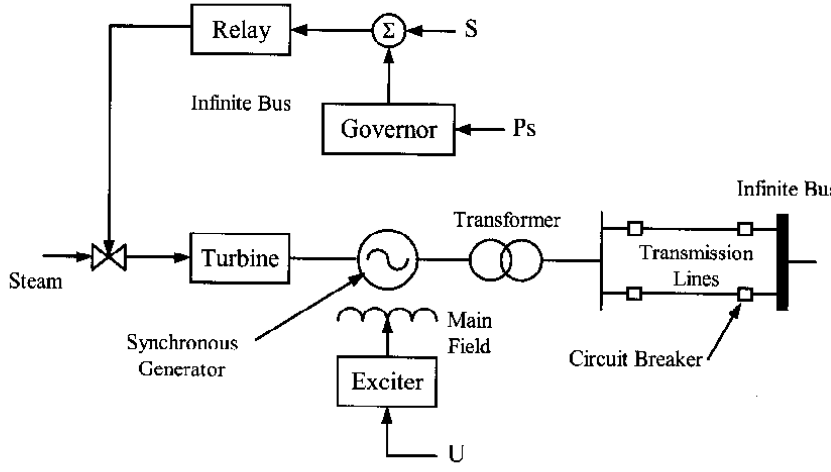


**Fig. 1. Schematic diagram of power system considered.**

## Proposed Scheme

A block diagram of an artificial neural network based power system stabilizer for synchronous machine excitation control connected to an infinite bus via a transformer and transmission lines is shown in Fig. 2. Thc artificial neural network power system stabilizer (ANNPSS) is fed by the speed error deviation ($\Delta\omega$) and the incremental change in machine terminal voltage ($\Delta V_t$). The output of the ANNPSS is fed with the voltage reference and the terminal voltage to the excitation system of the synchronous machine.

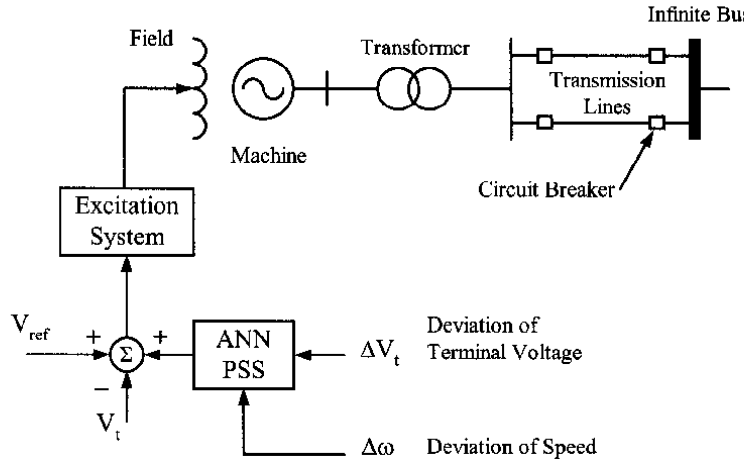


**Fig. 2. Schematic diagram of one machine infinite bus system and ANNPSS.**

## Simulation System Studies

The proposed artificial neural network based power system stabilizer model for synchronous machine excitation control is illustrated in Fig. 3. Here, a synchronous machine with standard governor and excitation control is connected to an infinite bus. The input ($U_t$) refers to the input to the exciter and the output (Y) could be the rotor speed (frequency) and the voltage of the machine.

The output of the classical stabilizer was chosen as an input. $Y_d$ refers to the desired output of the stabilizer. The system measurements vector X referred to in Fig. 3 can include the exciter voltage, machine angle, rotor speed, turbine torque, steam power, and exciting flux. The signals of the system measurements are to be adapted as input signals to the ANN controller. The latter uses the Levenberg-Marquardt back propagation algorithm to train the network to reduce the error between machine output Y and desired output $Y_d$. The ANN controller produces an output signal U to control the machine excitation system level to keep the machine at the desired operating position.

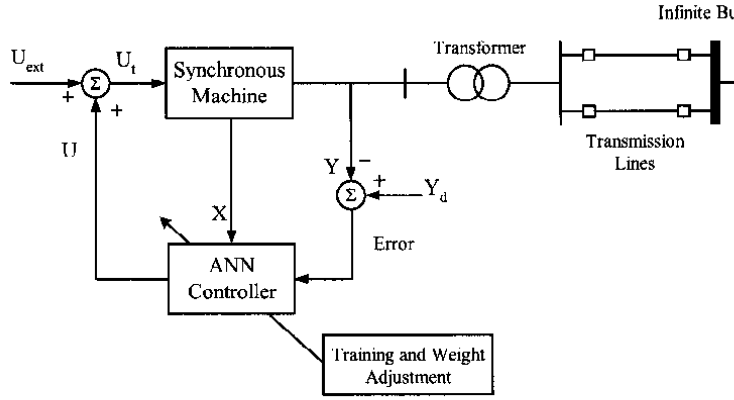


**Fig. 3. ANNPSS controller for synchronous machine excitation control.**

## Architecture of ANNPSS

The artificial neural network based power system stabilizer used in this paper is shown in Fig. 4. The neural network used is a feed-forward multilayer network, and it consists of two layers. The first layer is a hyperbolic tangent sigmoid (tansig) and the second layer is a pure linear (purelin) of fully connected processing elements which map inputs from the continuous domain to outputs normalized to a range of (0.0 to 1.0). This neural network is chosen because it can be trained to approximate most functions arbitrarily well. The input layer consists of two neurons (speed and voltage deviations). The tansig hidden layer has eight neurons and the pure linear output layer has only one neuron for the $U_{PSS}$ output. The number of hidden layers and the neurons in each layer are subject to the complexity of the mapping, computer memory, computation time and the desired control effect. Too many neurons result in a waste of computer memory and computation time, while too few neurons may not provide the desired control effect. The more complicated the input-output mapping, the more neurons are needed. Due to the non-linearity of the power systems, two hidden layers are selected [14-15].

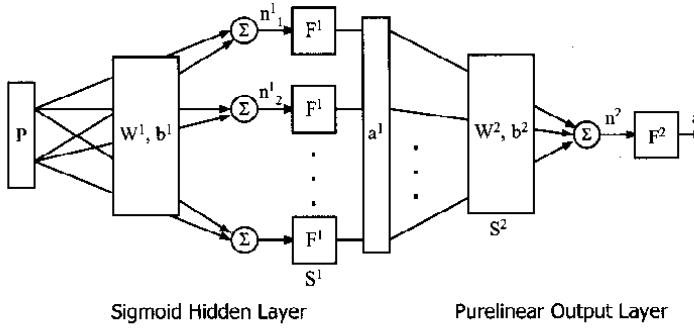


**Fig. 4. Two-layer ANN-based PSS.**

In Fig. 4, P depicts the network input vector = ($\Delta V_t$ , $\Delta\omega$) and $a^2$ depicts the ANNPSS output $U_{PSS}$. Superscript indicates order of layer, i.e. first layer or second layer. For example, $S^1$ and $S^2$ are number of neurons in hidden and output layers, respectively. The hidden layer activation function $F^1$ is chosen to be hyperbolic tangent sigmoid (tansig) defined by

$$a_i = F(n_i) = (e^{n_i} - e^{-n_i})/(e^{n_i} + e^{-n_i}) \tag{1}$$

Each neuron has a combining function ($n_i$) that is the weighted sum of the inputs to that neuron, i.e.

$$n_i = \sum_k (W_{ik} P_k) \tag{2}$$

where k = 1, 2, ... , S and S is the number of neurons in layer. In computing the activation value of each neuron all the weights in the network are first set to random values ($W_1$, $b_1$) and ($W_2$, $b_2$).

The Levenberg-Marquardt back propagation algorithm is used for training the artificial neural network power system stabilizer (ANNPSS) because it is faster than the ordinary back propagation algorithm. The Levenberg-Marquardt back propagation algorithm [16,17] can be summarized in the following steps:

1. Present all inputs to the network and compute the corresponding network outputs, using the equations:

$$S_i^m = \frac{\partial \hat{F}}{\partial n_i^m} \equiv \frac{\partial e_q^T e_q}{\partial n_i^m} \tag{3}$$

$$\tilde{S}_{i,h}^m \equiv \frac{\partial v_h}{\partial n_{i,q}^m} = \frac{\partial e_{k,q}}{\partial n_{i,q}^m} \tag{4}$$

2. Compute the errors using the relation:

$$e_q = t_q - a_q \tag{5}$$

3. Compute the sum of squared errors over all inputs F(x) by the equation:

$$\begin{aligned} F(x) &= \sum_{q=1}^{Q} (t_q - a_q)^T (t_q - a_q) \\ &= \sum_{q=1}^{Q} e_q^T e_q = \sum_{q=1}^{Q} \sum_{j=1}^{S^M} (e_{j,q})^2 = \sum_{i=1}^{N} (v_i)^2 \end{aligned} \tag{6}$$

4. Compute the Jacobian matrix by the equation:

$$J(x) = \begin{bmatrix} \frac{\partial e_{1,1}}{\partial w^1_{1,1}} & \frac{\partial e_{1,1}}{\partial w^1_{1,2}} & \cdots & \frac{\partial e_{1,1}}{\partial w^1_{S^1,R}} & \frac{\partial e_{1,1}}{\partial b^1_1} & \cdots \\ \frac{\partial e_{2,1}}{\partial w^1_{1,1}} & \frac{\partial e_{2,1}}{\partial w^1_{1,2}} & \cdots & \frac{\partial e_{2,1}}{\partial w^1_{S^1,R}} & \frac{\partial e_{2,1}}{\partial b^1_1} & \cdots \\ \vdots & \vdots & \cdots & \vdots & \vdots & \cdots \\ \frac{\partial e_{S^M,1}}{\partial w^1_{1,1}} & \frac{\partial e_{S^M,1}}{\partial w^1_{1,2}} & \cdots & \frac{\partial e_{S^M,1}}{\partial w^1_{S^1,R}} & \frac{\partial e_{S^M,1}}{\partial b^1_1} & \cdots \\ \frac{\partial e_{1,2}}{\partial w^1_{1,1}} & \frac{\partial e_{1,2}}{\partial w^1_{1,2}} & \cdots & \frac{\partial e_{1,2}}{\partial w^1_{S^1,R}} & \frac{\partial e_{1,2}}{\partial b^1_1} & \cdots \\ \vdots & \vdots & \cdots & \vdots & \vdots & \cdots \end{bmatrix} \tag{7}$$

5. Initialise for computing the sensitivities with the equation:

$$\tilde{S}^M_q = -\dot{F}^M(n^M_q) \tag{8}$$

6. Calculate the sensitivities with the recurrence relations by the equation:

$$\tilde{S}^m_q = \dot{F}^m(n^m_q)(W^{m+1})^T \tilde{S}^{m+1}_q \tag{9}$$

7. Augment the individual matrices into the Levenberg-Marquardt sensitivities by the quation:

$$\tilde{S}^m = \left[ \tilde{S}^m_1 \middle| \tilde{S}^m_2 \middle| \cdots \middle| \tilde{S}^m_Q \right] \tag{10}$$

8. Compute the elements of the Jacobian matrix by the equations:

$$[J]_{h,l} = \frac{\partial v_h}{\partial x_l} = \frac{\partial e_{k,q}}{\partial w^m_{i,j}} = \frac{\partial e_{k,q}}{\partial n^m_{i,q}} \frac{\partial n^m_{i,q}}{\partial w^m_{i,j}} = \tilde{S}^m_{i,h} \frac{\partial n^m_{i,q}}{\partial w^m_{i,j}} = \tilde{S}^m_{i,h} a^{m-1}_{j,q} \tag{11}$$

$$[J]_{h,l} = \frac{\partial v_h}{\partial x_l} = \frac{\partial e_{k,q}}{\partial b^m_i} = \frac{\partial e_{k,q}}{\partial n^m_{i,q}} \frac{\partial n^m_{i,q}}{\partial b^m_i} = \tilde{S}^m_{i,h} \frac{\partial n^m_{i,q}}{\partial b^m_i} - \tilde{S}^m_{i,h} \tag{12}$$

9. Solve to obtain $\Delta x_k$ using equation:

$$\Delta x_k = -[J^T(x_k)J(x_k) + \mu_k I]^{-1} J^T(x_k) v(x_k) \tag{13}$$

10. Re-compute the sum of squared errors, using $x_k+\Delta x_k$. If this new sum of squares is smaller than computed in step 1, divide $\mu_k$ by some factor $\alpha > 1$ (typically, $\alpha = 10$). Let $x_{k+1} = x_k + \Delta x^k$ and go back to step 1. If the sum of squares is not reduced, then multiply $\mu_k$ by $\alpha$ and go back to step 3.

11. The algorithm is assumed to have converged when the norm of the gradient:

$$\nabla F(x) = 2 J^T(x) v(x) \qquad (14)$$

is less than some predetermined value, or when the sum of squares has been reduced to some error goal.

The data input-output pairs required for off-line training are obtained by running the selected simulation model of Fig. 4 at load levels (10 , 20, 30, 40, 50, 60, 70 ,80, 90, and 100%) with (5%) disturbance in the setting of the governor followed by (5%) disturbance in the reference voltage. The same load levels have been chosen to obtain the data for off-line training for faulted conditions. The testing data are obtained by the same procedure as the training data except that the load levels are chosen at (5, 15, 25, 35, 45, 55, 65, 75, 85, and 95%). The Neural Network Toolbox and Simulink software packages [18] were used for simulation, training and testing the designed artificial neural network based power system stabilizer.

## Results

The sum-squared network training error curve is shown in Fig. 5. The training procedure used variable learning rate (0.001, 0.0001 and 0.00001). The performance of the artificial neural network based power system stabilizer was tested and compared with the response of the classical power system stabilizer. Due to the huge number of characteristic curves, which are obtained as a result of training and testing the different models, only selected results will be shown. These are the results of testing ANNPSS at normal operating conditions and faulted cases under the disturbances of (+5%) in governor setting followed by (+5 %) in reference voltage at load level (95%) of full load as shown in Fig. 6. From the characteristic curves of testing ANNPSS, it is noticed that the ANNPSS has less overshooting, less rotor power angle and higher terminal voltage in comparison with the conventional (classical) power system stabilizer PSS.

The simulation results can be summarized as follows:

(I) At load (0.95 pu) of full load (normal operating conditions, Fig. 6):

- Oscillations in angular speed with 0.4% overshooting and decay within 5 seconds.
- Oscillations in rotor angel with 1.4% overshooting and decay within 5 seconds.
- Oscillations in terminal voltage with 0.025% overshooting and decay within 4 seconds.

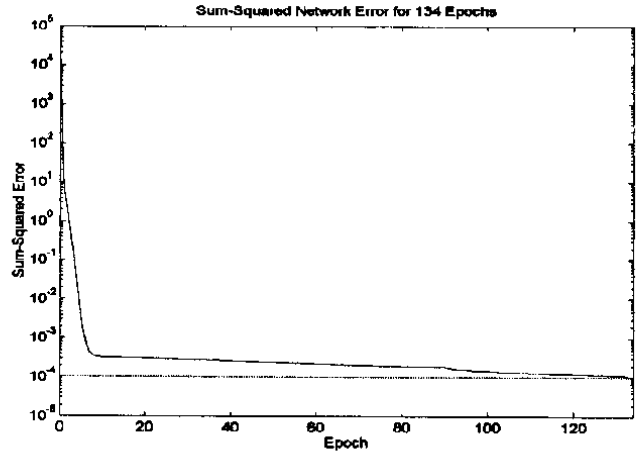


**Fig. 5. Sum squared error for the trained neural network.**

It is evident from the simulation curves of Fig. 6 that the value of the rotor angle for the ANNPSS is 0.018% which is less than its value in the case of classical PSS. But the value of the terminal voltage for the ANNPSS is 0.024% which is higher than its value in the case of classical PSS.

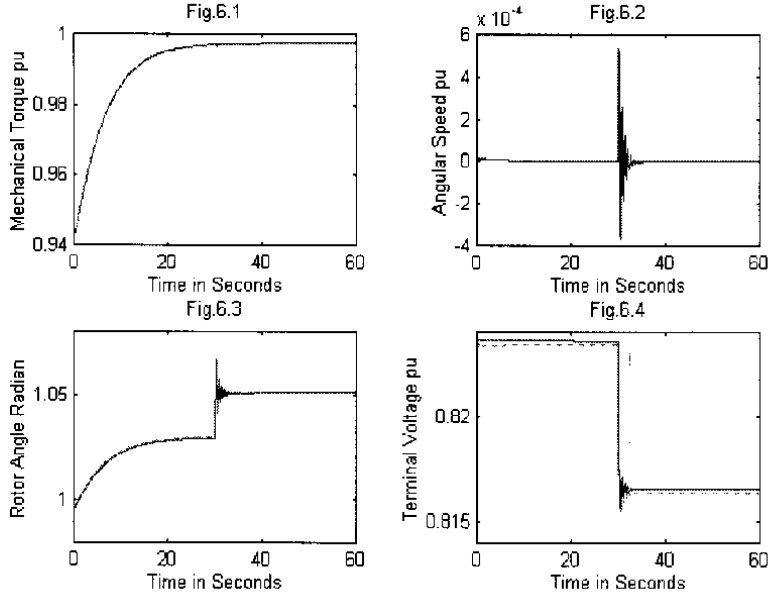


**Fig. 6. Simulation curves due to +5% in the governor setting followed by +5% in the voltage reference (solid line = ANNPSS, dashed line = PSS).**

(II) At load (0.95 pu) of full load (faulted case, Fig. 7):

- Oscillations in angular speed with 0.6% overshooting and decay within 5 seconds.
- Oscillations in rotor angel with 1.8% overshooting and decay within 5 seconds.
- Oscillations in terminal voltage with 0.03% overshooting and decay within 4 seconds.

It is evident from the simulation curves of Fig. 7 that the value of the rotor angle in case of ANNPSS is 0.023% less than its value in the case of classical PSS. But the value of the terminal voltage in the case of ANNPSS is 0.029% higher than its value in the case of classical PSS.

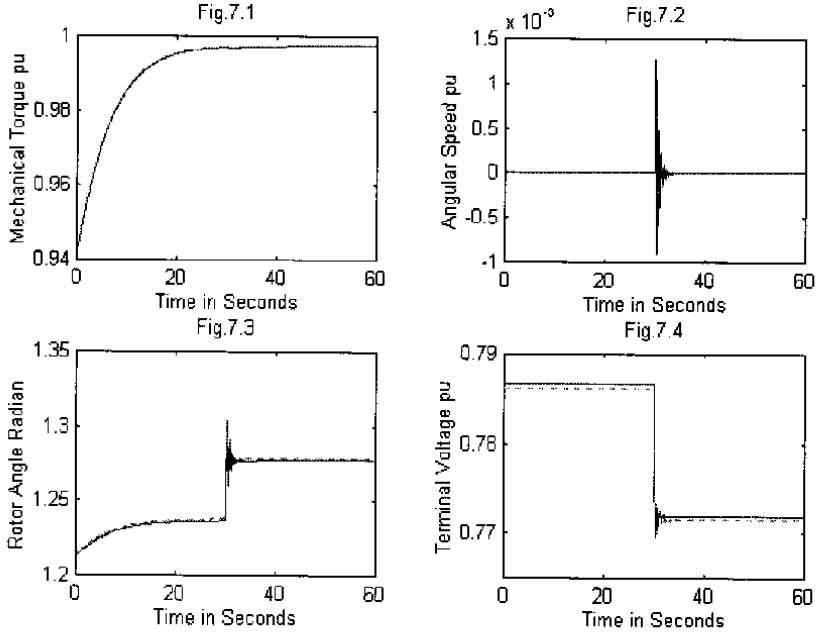


**Fig. 7. Simulation curves due to +5% in the governor setting followed by +5% in the voltage reference (solid line = ANNPSS, dashed line = PSS).**

From the above results, it can be seen that the artificial neural network based power system stabilizer (ANNPSS) not only mimics the conventional power system stabilizer (PSS) but it renders an improved performance, especially at the faulted cases of different load levels. This is quite interesting in the light of the fact that the conventional PSS data was used to train the ANNPSS.

## Conclusion

Two stabilizers, conventional power system stabilizer and artificial neural network based power system stabilizer, have been studied and their effect in controlling a 300 MW turbo-generator has been compared. The test results have indicated that the artificial neural network based power system stabilizer provides an improved performance compared to that of the conventional power system stabilizer over a wide range of normal and faulted operating conditions and disturbances. This can be attributed to the advantages of artificial neural networks. Such networks have the ability of synthesizing complex and non-linear systems. The ANNPSS has adaptively adjusted to new operating conditions quite easily, providing a more direct solution to a highly non-linear and complex control problem. The computational cost and hardware requirements in terms of memory and central processing unit time are not extensive for the tested cases.

## References

[1] Jones, G.A. "Phasor Interpretation of Generator Supplementary Excitation Control". *The IEEE Summer Power Meeting*, San Francisco: California, Paper # A75-473-4, 1975.

[2] de Mello, F. and Concordia, C. "Concepts of Synchronous Machine Stability as Affected by Excitation Control". *IEEE Transactions PAS*, 89, No. 4 (April 1969), 316-329.

[3] Anderson, P. and Fouad, A. *Power System Control and Stability*, The Iowa State University Press, U.S.A., 1981.

[4] Yu, Y-N. *Electric Power System Dynamics*, New York: Academic Press, 1983.

[5] de Mello, F., Nolan, P., Laskowski, T. and Undrill, J. "Coordinated Application of Stabilizers in Multi-machine Power System". *IEEE Transactions PAS*, 99 (1980), 892-901.

[6] Larsen, E. and Swarm, D. "Applying Power System Stabilizer". *IEEE Transactions PAS*, 100 (1977), 3017-3046.

[7] Ishgura, F., Tanaka, S., Shimomura, M., Meada, T., Matsushita, K. and Sugimoto, H. "Coordinated Stabilizing Control Exciter, Turbine and Breaking Resistor". *IEEE Transactions PWRS*, 1 (1986), 74-80.

[8] Wilson, W.J. and Aplevich, J.D. "Coordinated Governor/exciter Stabilizer Design in Multi-machine Power Systems". *IEEE Transactions on Energy Conversion*, 1 (1986), 61-67.

[9] Hsu, Y., and Su, C. "Application of Power System Stabilizer on a Power System with Pumped Storage Plant". *IEEE Transactions PS*, 3 (1988), 80 86.

[10] Hsu, Y., and Wu, C. "Adaptive Control of a Synchronous Machine Using Auto-searching Method". *IEEE Transactions on PWRS*, 3 (1988), 1434-1440.

[11] Raflan, M., Sterling, M. and Irving, M. "Real-time Power System Simulation". *Proc. IEE, Part C*, 134, No. 3 (May, 1987), 206-233.

[12] Saidy, M. and Hughes, F.M. "An Extended Block Diagram Transfer Function Model of a Synchronous Machine". *Electrical Power & Energy Systems*, 18, No. 2 (1996), 139-142.

[13] Foda, S.G., El-Sayed, M.A. and Abou-Elenein, A.N. "Performance Comparison of Different Control Models for Large Synchronous Generator". The *Kuwait Journal of Science & Engineering*, 26, No. 1 (1999), 49-67.

[14] Zhang, Y., Malik, O.P., Hope, G.S. and Chen, G.P. "Application of an Inverse Input/output Mapped ANN as a Power System Stabilizer" *IEEE/PES Winter Meeting* (93 WM 130-5 EC), 1993.

[15] Zhang, Y., Malik, O.P. and Chen, G.P. "Artificial Neural Network Power System Stabilizers in Multi-machine Power System Environment" *IEEE Transactions on Energy Conversion*, 10, No. 1 (March, 1995), 147-155.

[16] Rumelhart, D.E., Hinton, G.E. and Williams, R.J. "Learning Internal Representation by Error Propagation". In: *Parallel Data Processing*, D. Rumelhart and J. MeClelland, (Ed.), Cambridge MA: MIT Press, 1986.

[17] Hagan, M.T., Demuth, H.B. and Beale, M. *Neural Network Design*, Boston MA: PWS Publishing Company, 1996.

[18] Demuth, H. and Beale, M. *Neural Network TOOLBOX for Use with Matlab, the MathWorks Inc.*, 1994.

# تصميم موازنات نظم القدرة باستخدم الشبكات الحاسوبية العصبية للمولدات المتزامنة الضخمة

**صلاح جاد فودة**

*قسم الهندسة الكهربية ، كلية الهندسة ، جامعة الملك سعود، ص.ب. ٨٠٠، الرياض ١١٤٢١ ، المملكة العربية السعودية*

(قدّم للنشر في ٢٠٠٠/١١/٤م ؛ وقبل للنشر في ٢٠٠١/٥/٨م)

**ملخص البحث.** يعرض هذا البحث موازنا لنظم القدرة الكهربية مبنيا على أساس شبكات الحاسوب العصبية للتحكم فى نظام إثارة مولد تزامني. ويعمل المولد تحت ظروف تشغيل متعددة وقد خضع لأنواع مختلفة من ظروف التشغيل الطارئة. واختير مولد تزامنى بقدرة ٣٠٠ ميجاوات للحصول على معلومات تدريب المتحكم الشبكي الحاسوبي العصبي. وقد استعملت طريقة المحاكاة الحاسوبية للمولد مع موازن تقليدي تحت ظروف التشغيل المختلفة للحصول على البيانات الداخلة والخارجة المستعملة فى التدريب. واستعمل موازن نظام القدرة الحاسوبي العصبي المصمم باستخدام شبكات التغذية العكسية المتعددة الطبقات لبناء موازن عصبي بديل، حيث اختير حيدان سرعة المولد الزاوية والتغير في جهده كمدخلات للمتحكم الحاسوبي العصبي. وعقدت مقارنة بين أداء الموازن التقليدي والموازن العصبي وبينت أفضلية الموازن المقترح من حيث التأقلم والمرونة والأداء تحت ظروف التشغيل المتعددة.